### Title

Environmental formation of methylmercury is controlled by synergy of inorganic mercury bioavailability and microbial mercury-methylation capacity




### Journal

Environmental Microbiology, 25(8)

### ISSN

1462-2912



### Authors

Peterson, Benjamin D
Krabbenhoft, David P
McMahon, Katherine D
et al.



### Publication Date

2023-08-01

### DOI

10.1111/1462-2920.16364

# Environmental formation of methylmercury is controlled by synergy of inorganic mercury bioavailability and microbial mercury-methylation capacity

Benjamin D. Peterson (bdpeterson@ucdavis.edu)[1,2*], David P. Krabbenhoft (dpkrabbe@usgs.gov)[3], Katherine D. McMahon (trina.mcmahon@wisc.edu)[1,4], Jacob M. Ogorek (jmogorek@usgs.gov)[3], Michael T. Tate (mttate@usgs.gov)[3], William H. Orem (borem@usgs.gov)[5], Brett A. Poulin (bapoulin@ucdavis.edu)[2]

1. Department of Bacteriology, University of Wisconsin - Madison, Madison, WI 53706, United States
2. Department of Environmental Toxicology, University of California - Davis, Davis, CA 95616, United States
3. U.S. Geological Survey, Upper Midwest Water Science Center, Mercury Research Laboratory, Madison, Wisconsin 53726, United States
4. Department of Civil and Environmental Engineering, University of Wisconsin - Madison, Madison, Wisconsin 53706, United States
5. U.S. Geological Survey, Geology, Energy & Minerals Science Center, Reston, Virginia 20192, United States

* Corresponding author

Ethics and integrity policies: All metagenomic, incubation, and geochemical data are available as

22 supplemental data or online, as outlined in the methods section. Funding sources are described at

23 the end of the manuscript. All authors declare no conflict of interest.

## Abstract

Methylmercury (MeHg) production is controlled by the bioavailability of inorganic divalent mercury ($Hg(II)_i$) and Hg-methylation capacity of the microbial community (conferred by the *hgcAB* gene cluster). However, the relative importance of these factors and their interaction in the environment remain poorly understood. Here, metagenomic sequencing and a full-factorial MeHg formation experiment were conducted across a wetland sulfate gradient with different microbial communities and pore water chemistries. From this experiment, the relative importance of each factor on MeHg formation was isolated. $Hg(II)_i$ bioavailability correlated with the dissolved organic matter composition, while the microbial Hg-methylation capacity correlated with the abundance of *hgcA* genes. MeHg formation responded synergistically to both factors. Notably, *hgcA* sequences were from diverse taxonomic groups, none of which contained genes for dissimilatory sulfate reduction. This work expands our understanding of the geochemical and microbial constraints on MeHg formation *in situ* and provides an experimental framework for further mechanistic studies.

## Originality/Significance Statement

While inorganic mercury ($Hg(II)_i$) bioavailability and mercury-methylation capacity of microbial communities are both known to influence methylmercury (MeHg) production in the environment, direct comparisons of these two factors under environmental conditions have not been done. In this study, we used a full-factorial experimental design with intact peat cores and pore waters pre-equilibrated with $Hg(II)_i$ to directly compare these two factors under environmentally relevant conditions. Using this approach, we showed that either $Hg(II)_i$ bioavailability or microbial mercury-methylation capacity can be the limiting factor under environmental conditions. We also paired these incubations with comprehensive geochemical characterization of the pore water matrices and shotgun metagenomic sequencing of the microbial communities in the peat. This showed that dissolved organic matter controlled $Hg(II)_i$ bioavailability more than sulfide concentrations and the abundance of the *hgcA* gene within the microbial community was linked closely to the microbial mercury-methylation capacity. These insights were only possible due to this novel and interdisciplinary approach. This work provides a framework for future studies to investigate the relative roles of $Hg(II)_i$ bioavailability and microbial methylation capacity, as well as the biogeochemical parameters that drive them, under environmentally relevant conditions.

## Introduction

Methylmercury (MeHg) is the most toxic and bioaccumulative form of mercury (Hg) in the environment (Wiener et al., 2003) and poses significant health risks to humans, fish, and wildlife worldwide. MeHg formation by microbes in the environment occurs primarily under low-redox conditions and is dependent on the bioavailability of inorganic divalent Hg ($Hg(II)_i$) and the Hg-methylating capacity of the microbial community (Hsu-Kim et al., 2013). The geochemical constraints on $Hg(II)_i$ bioavailability for microbial uptake are controlled by ligand complexation of $Hg(II)_i$ by primarily organic and inorganic reduced S (Graham et al., 2013; Hsu-Kim et al., 2013, p.; Poulin, Gerbig, et al., 2017), whereas $Hg(II)_i$ methylation capacity is conferred by the presence of the *hgcAB* gene cluster (Gilmour et al., 2013; Parks et al., 2013). Previous studies individually investigated the importance of $Hg(II)_i$ bioavailability (Graham et al., 2013; Hsu-Kim et al., 2013; Jonsson et al., 2012) or microbial communities (Christensen et al., 2018; Compeau & Bartha, 1985; Gilmour et al., 1992; Schaefer et al., 2020) to MeHg formation. In amended sediment slurries with simplified ligand chemistries, neither $Hg(II)_i$ bioavailability nor overall microbial activity were strictly limiting; rather, each was shown to influence MeHg production under different conditions (Kucharzyk et al., 2015). In anoxic brackish waters, gene abundance or expression of *hgcA* combined with predicted abundance of $Hg(II)_i$-sulfide species correlated to MeHg production potentials (Capo, Feng, et al., 2022). Expanding this body of work to a simultaneous quantitative examination of the relative importance of geochemical versus microbial factors to MeHg formation in complex environmental systems, paired with comprehensive measurements of the ligand chemistry and

78 microbial Hg-methylators, is a critical step in understanding environmental MeHg production
79 and has not yet been done.
80 Ligand complexation and geochemical speciation of $Hg(II)_i$ ultimately govern $Hg(II)_i$
81 availability for uptake by microbial cells (Hsu-Kim et al., 2013, p.), which can have long-lasting
82 effects on Hg methylation (Jonsson et al., 2012) and incorporation into the food web (Jonsson et
83 al., 2014). Under environmental conditions lacking inorganic sulfide, $Hg(II)_i$ is exclusively
84 bound to thiol groups ($S_{Red}$) in dissolved organic matter (DOM) (Haitzer et al., 2002).
85 Conversely, under sulfidic conditions common in anoxic sediments, nano-particulate β-HgS
86 dominates $Hg(II)_i$ speciation (Gerbig et al., 2011; Poulin, Gerbig, et al., 2017). The
87 bioavailability of $Hg(II)_i$ associated with nano-particulate β-HgS is greatest at low-to-
88 intermediate sulfide concentrations ( ≤ ~0.3 mg/L) and in the presence of DOM of high
89 aromaticity (Graham et al., 2013) and thiol content (Graham et al., 2017). Under very high
90 sulfide concentrations (>~3 mg/L), nano-particulate β-HgS becomes crystalline and aggregates
91 (Poulin, Gerbig, et al., 2017), decreasing $Hg(II)_i$ bioavailability for methylation (T. Zhang et al.,
92 2012). Further, sulfidic conditions enhance the concentration of thiol groups in DOM via
93 sulfurization reactions (Poulin, Ryan, et al., 2017; Vairavamurthy & Mopper, 1987), which
94 enhances the bioavailability of $Hg(II)_i$ to methylation (Bouchet et al., 2018; Graham et al., 2017).
95 However, the net effect of sulfide vs. DOM composition and concentration on bioavailability of
96 $Hg(II)_i$ in complex environmental systems is still unclear. In pure culture, efforts to minimize the
97 geochemical complexity of study systems has relied on the use of cysteine as a low-molecular
98 weight analogue to thiols in DOM, which promotes the bioavailability of $Hg(II)_i$ under
99 laboratory conditions (Gilmour et al., 2018; Graham et al., 2012; Schaefer & Morel, 2009).

However, the environmental relevance of cysteine controlling the bioavailability of $Hg(II)_i$ has yet to be tested.

The environmental factors controlling the microbial Hg-methylation capacity are poorly understood. Sulfate-reducing bacteria (SRB) have long been considered a primary microbial guild affiliated with MeHg production due to field experiments under molybdate inhibition (Compeau & Bartha, 1985) or sulfate amendment (Gilmour et al., 1992). However, using the *hgcAB* gene cluster as a molecular marker (Parks et al., 2013), we now recognize the high metabolic and phylogenetic diversity of putative Hg-methylating organisms (Gilmour et al., 2013; Gionfriddo et al., 2016; McDaniel et al., 2020; Podar et al., 2015). Several recent field studies in sulfate-enriched environments observed that SRB accounted for only a small percentage of the *hgcA* abundance, while the majority of *hgcA* abundance was associated with fermentative and syntrophic bacteria or methanogenic archaea (Bae et al., 2014; Jones et al., 2019, 2020; Peterson et al., 2020). Attempts to link *hgcA* abundance to MeHg levels or production have met with mixed results, possibly due to $Hg(II)_i$ bioavailability, limited methodologies, and/or changes in *hgcA* expression/HgcA activity (Bae et al., 2019; Bravo et al., 2016; Christensen et al., 2019; Liu et al., 2018; Millera Ferriz et al., 2021; Roth et al., 2021; Tada et al., 2020). Complex biogeochemical conditions and interdependent microbial communities in the environment also make it difficult to extend observations from laboratory culture studies (Gilmour et al., 2013, 2018; Yu et al., 2018) to natural conditions and anticipate which microbial processes are linked to MeHg production. These complexities may explain the varied response of MeHg production to experimental molybdate inhibition (Bae et al., 2014; Bouchet et al., 2018; Cleckner et al., 1999; Gascón Díez et al., 2016; Schaefer et al., 2020) or sulfate amendment (Gilmour et al., 1992; Jones et al., 2020). Overall, the relationships between

123 microbial community metabolism, *hgcA* gene content/activity, Hg-methylation capacity of the
124 microbial community, and ultimately MeHg production and accumulation are still poorly
125 understood.

126 To address these knowledge gaps, we quantified the relative importance of $Hg(II)_i$
127 bioavailability and microbial Hg-methylation capacity on MeHg formation across a sulfate
128 gradient in the Florida Everglades and paired that with microbial community characterization
129 and pore water chemistry characterization. First, a full-factorial MeHg formation experiment was
130 performed using pore waters and intact peat cores collected at six sites across a sulfate gradient
131 to quantify the relative methylation potential of both the pore water and microbial communities
132 in the peat. Next, shotgun metagenomic sequencing was performed to quantify and characterize
133 the microbial community fraction carrying the *hgcA* gene. Together, these complementary
134 approaches facilitated the isolation of geochemical factors governing $Hg(II)_i$ bioavailability from
135 the microbial Hg-methylation capacity (i.e., *hgcA* abundance). Furthermore, genome-resolved
136 metagenomic analyses identified the metabolic potential of microbes with *hgcA* in the peat cores.
137 This study demonstrates the synergy between geochemical and microbial factors required for
138 environmental MeHg formation, shows that *hgcA* gene abundance is a reliable marker for the
139 Hg-methylation capacity of the microbial community, and provides a valuable experimental
140 framework to target processes underlying MeHg formation in diverse aquatic environments.

## Materials and methods

**Site information and geochemical gradients:** The Florida Everglades (USA) is an ideal "field laboratory" to study the impact of sulfate concentration and DOM concentration/composition on MeHg production due to the combination of extensive atmospheric Hg deposition (Krabbenhoft et al., 1998; Orem et al., 2020) with long-term geochemical gradients stemming from release points of agricultural run-off (Fig. S1) (Orem et al., 2011). In this study, six field sites in Water Conservation Areas 2 (WCA-2) and 3 (WCA-3) and Arthur R. Marshall Loxahatchee National Wildlife Refuge (LOX), were chosen (Table S1; Fig. S1) to span a range of sulfate, sulfide, and DOM concentration and composition (Fig. S2). Ambient MeHg concentrations in the peat were lowest in WCA-2, intermediate at the downgradient sites in WCA-3, and highest at 3A-F and LOX8 (Fig. 1a). Ambient pore water MeHg concentrations were similarly low at WCA-2, but relatively consistent concentrations were observed across WCA-3 and LOX8 (Fig. 1b). Geochemical data and analytical methods are available in Science Base (Tate et al., 2023).

**MeHg Formation Assays:** Details for all materials and methods are provided in the Supporting Information. Briefly, at each of the six sites, filtered pore waters and 18 peat cores (7.6 cm diameter) were collected (Fig. S1). A suite of water quality and geochemical measurements, including sulfide, sulfate, DOC concentration, and DOM specific ultraviolet absorbance at 254 nm ($SUVA_{254}$), were made on the pore waters using established methods (Fig. S2, S3) (Poulin, Ryan, et al., 2017). Three laboratory-prepared "pore waters" were prepared using purged ultrapure water, all with a background solution matched to the average ionic concentration of Everglades pore water, including 1 mg/L sulfate: "F1 DOM HPOA", which

contained 90 mg/L of the hydrophobic organic acid fraction (HPOA) of DOM from the F1 site of the Everglades (Poulin, Ryan, et al., 2017); "Cysteine", with 40 µM of cysteine; and "Control", which had no additional organic ligands. The $^{201}Hg(II)_i$ tracer was pre-equilibrated with each of the filtered natural and lab-prepared pore waters for a minimum of 4 hours. From each of the six field sites, duplicate peat cores were injected with one of the nine different pore water-equilibrated $^{201}Hg(II)_i$ tracers in a full-factorial experimental design, for a total of 108 incubations (Fig. S4). 1.5 ml of equilibrated tracer was injected every 1 cm from 2 cm to 10 cm below the top of the core. Injection concentrations were targeted such that the $^{201}Hg(II)_i$ concentration in the peat would be 13% of the ambient HgT. After 24 hours, the peat cores were frozen to stop the experiment and shipped back to the laboratory on dry ice. The top 2 cm of the core (mostly biofilm) was removed, and the next 4 cm (solid peat) were homogenized for analysis. This was previously shown to be a highly active zone of MeHg production (Gilmour et al., 1998). Excess $Me^{201}Hg$ was quantified by distillation and isotope dilution with inductively coupled plasma mass spectroscopy (ICP-MS; iCAP, Thermo Scientific) (DeWild et al., 2002; Hintelmann & Evans, 1997), while excess total $^{201}Hg$ ($^{201}HgT$) was measured using BrCl oxidation, $SnCl_2$ reduction, and ICP-MS (Hintelmann & Evans, 1997; Olund et al., 2004). Net $Me^{201}Hg$ production (NMP) was defined as follows: NMP = excess $Me^{201}Hg$ / excess $^{201}HgT$ * 100. Relative methylation potential values were calculated for the pore water ($RMP_{matrix}$) and the peat cores ($RMP_{peat}$) by normalizing net $Me^{201}Hg$ production to the highest net $Me^{201}Hg$ production value for any incubation using the same peat core or pore water, respectively (Fig. S4). A synchronized permutation test using the two-way analysis of variance format (Basso et al., 2009) with log-transformation was done to test for main and interaction effects of the peat core and pore water source on net $Me^{201}Hg$ production. Model selection was done using Akaike Information Criteria

on linear models generated using different combinations of factors. Linear models were used to test for relationships between combinations of $RMP_{matrix}$, $RMP_{peat}$, geochemical parameters, and *hgcA* abundance. Incubation data are available in Table S2.

**Metagenomics workflow**: DNA was isolated from the peat by phenol:chloroform extraction and purified by alcohol precipitation (Lever et al., 2015) then sequenced at QB3 Genomics at the University of California, Berkeley (Berkeley, CA). DNA reads from duplicate metagenomes were coassembled using both metaSPADes and MegaHit (Li et al., 2015; Nurk et al., 2017) and open reading frames were predicted from the assembled contigs using Prodigal (Hyatt et al., 2010). HgcA sequences were identified using a custom Hidden Markov Model (Peterson et al., 2020) and manually verified to contain conserved domains (Parks et al., 2013), then dereplicated across assemblies using CD-HIT (Fu et al., 2012). Confirmed HgcA sequences were aligned with the Hg-MATE database (Gionfriddo et al., 2021, p.) and a maximum-likelihood tree was generated using RAxML (Stamatakis, 2014). This, along with a custom workflow (Gionfriddo et al., 2020, p. 20), was used to assign a taxonomic affiliation to each *hgcA* gene. Normalized abundance of *hgcA* was calculated by first determining the average nucleotide coverage over the *hgcA*-containing contig, then dividing this by the mean coverage of 16 single-copy ribosomal proteins (Sorek et al., 2007). Thus, the normalized *hgcA* abundance is presented as a percentage of the total microbial community. Genomic bins containing *hgcA* were manually binned using CONCOCT (Alneberg et al., 2014) and refined in Anvi'o (Eren et al., 2015). These bins were taxonomically classified (Chaumeil et al., 2019) and their metabolic pathways identified (Zhou et al., 2022). Raw metagenomic reads are available through the National Center for Biotechnology Information under BioProject accession ID PRJNA808433 and the

assemblies, bins, and HgcA protein sequences are available through the Open Science Framework (https://osf.io/8muzf/). Code for all analyses and figures is stored on Github (https://github.com/petersonben50/Everglades).

## Results and Discussion

Net $Me^{201}Hg$ production in the peat core assays, quantified as the percent of excess $^{201}HgT$ measured as excess $Me^{201}Hg$, ranged from 0% to 8% after 24 hours across the six different peat cores incubated with nine pore water matrices ($n$=108 peat cores total; Fig. 1c, S5; Table S2). The inset in Fig. 1c shows how the effect of the two variables (peat core vs. pore water matrix source) on net $Me^{201}Hg$ production can be observed in the plot. Across all assays, the response of net $Me^{201}Hg$ production to the pore water matrix source, visualized as the spread between differently colored lines in Fig. 1c, was consistent regardless of the peat core source (Fig. 1c, S6). Changes in net $Me^{201}Hg$ production in response to the peat core source, visualized as the increase in net $Me^{201}Hg$ production along the x-axis, were less consistent depending on the pore water matrix, following one of two similar but distinct patterns, discussed in detail below (Fig. 1c, S7). Synchronized permutation testing (Basso et al., 2009) showed that both the peat core source ($p < 0.0001$) and the pore water matrix source ($p < 0.0001$) had significant effects on net $Me^{201}Hg$ production. There was also a statistically significant interaction effect ($p < 0.0001$). This interaction effect is visible in Fig. 1c in the two modestly different trends in the peat core effects depending on the source of the pore water matrix (Fig. 1c, S7). Four of the pore water matrices (Everglades F1 HPOA, 2A-N, 3A-O, and LOX8) facilitated a dramatic increase in net $Me^{201}Hg$ production in cores from sites 2A-A to 3A-O, but then net $Me^{201}Hg$ production leveled

off or modestly decreased in cores from sites WCA-3A and LOX8. In contrast, the other five pore water matrices resulted in modest increases in net $Me^{201}Hg$ production in cores from high to low sulfate, with a notable increase in net $Me^{201}Hg$ production in cores from sites 3A-F and LOX8 (Fig. 1c, S7). One possible source of this interaction is demethylation activity, which has been shown in isotopically enriched incubations after 8 hours in peat from the Everglades and would increase as $Me^{201}Hg$ concentrations increased (Gilmour et al., 1998). Another possibility is the complete methylation of the bioavailable pool of $^{201}Hg(II)_i$ in the high-producing incubations (Janssen et al., 2016). Either explanation is supported by the fact that pore water matrices that produce the plateau also produced the most $Me^{201}Hg$ and would result in an underestimation of Hg-methylation capacity, particularly at 3A-F and LOX8. Additional possible causes of this interaction effect are discussed in detail in the SI. Despite this interaction, the relative effects of each pore water matrix and peat core were notably consistent (Fig. 1c, S6, S7). Model selection identified a linear model without the interaction effect as the best fit for the data. Together, this suggests that the independent effects of the peat core and the pore water matrix had a much larger effect on net $Me^{201}Hg$ production than the interaction between them.

**Geochemical controls on $Hg(II)_i$ methylation:** The pore water matrix source had a significant and consistent influence on net $Me^{201}Hg$ production across the six peat cores (Fig. 1c, S6), likely by establishing the bioavailability of the $Hg(II)_i$ tracer, as demonstrated in previous studies (Gilmour et al., 1998; Graham et al., 2012, 2017; Jonsson et al., 2012, 2014; Moreau et al., 2015). Thus, the influence of the pore water matrix on net $Me^{201}Hg$ production reflects changes in $^{201}Hg(II)_i$ bioavailability due to ligand chemistry (Fig. S6). Regardless of the source of the peat

core, the Everglades F1 HPOA DOM solution yielded the most bioavailable $^{201}Hg(II)_i$, which is consistent with previous observations and attributed to the high aromaticity and thiol content of this DOM (Graham et al., 2013; Moreau et al., 2015; Poulin, Ryan, et al., 2017). Conversely, the control solution always resulted in the lowest net $Me^{201}Hg$ production. Surprisingly, the cysteine solution, which matched the thiol concentration of the Everglades F1 HPOA DOM, also resulted in exceptionally low net $Me^{201}Hg$ production, comparable to the control matrix. The net $Me^{201}Hg$ production of the six natural pore waters were distributed between that of the Everglades F1 HPOA DOM and the control matrix. Those collected from sites closest to where DOM and sulfate-rich canal water is released to the marshes (Sites 2A-N and 3A-O) consistently promoted the highest net $Me^{201}Hg$ production of the natural pore waters, whereas pore water from sites distant to canal inputs (e.g., Sites 2A-N and 3A-O) exhibited notably lower net $Me^{201}Hg$ production levels. LOX8 pore waters resulted in intermediate $Me^{201}Hg$ formation.

To quantify the variation in net $Me^{201}Hg$ production due to pore water matrix source for comparison to geochemical parameters, we calculated a "relative methylation potential" for each of the different pore water matrices ($RMP_{matrix}$) as follows. First, incubations were grouped by the source of the peat core; then, net $Me^{201}Hg$ production for each incubation was divided by the highest net $Me^{201}Hg$ production value of any incubation within the group (Fig. S4, S8). Of the measured geochemical properties of the natural and laboratory prepared pore water solutions (DOC, DOM $SUVA_{254}$, inorganic sulfide, UV absorbance), DOM $SUVA_{254}$ exhibited the strongest correlation with $RMP_{matrix}$ (adjusted $R^2 = 0.494$; $p < 0.001$; Fig. 2). Significant correlations with $RMP_{matrix}$ were also observed for DOC concentration (adjusted $R^2 = 0.405$; $p < 0.001$; Fig. S9a) and $UV_{254}$ absorbance (adjusted $R^2 = 0.376$; $p < 0.001$; Fig. S9b), the latter being a parameter that captures differences in both DOC concentration and DOM aromaticity. This is

consistent with extensive prior work showing that high aromatic DOM increases $Hg(II)_i$ bioavailability and facilitates MeHg formation in pure culture experiments (Graham et al., 2012, 2013; Moreau et al., 2015), as more aromatic DOM is not expected to stimulate microbial metabolism in the cores over the short timeframe of the experiments. Sulfide and $RMP_{matrix}$ were positively correlated, albeit weakly (adjusted $R^2 = 0.055$; $p = 0.008$; Fig. S9c). While it is known that high sulfide concentrations can inhibit MeHg production (Benoit et al., 1999; Graham et al., 2013) due to the formation of crystalline and aggregated β-HgS of low bioavailability (Poulin, Gerbig, et al., 2017; T. Zhang et al., 2012), aromatic DOM with high $S_{Red}$ content can inhibit crystalline β-HgS formation and promote $Hg(II)_i$ availability to methylation (Graham et al., 2017; Poulin, Ryan, et al., 2017). We interpret the high pore water $RMP_{matrix}$ from site 2A-N to indicate that even the highest sulfide concentration (3.5 mg/L) was insufficient to suppress $Hg(II)_i$ methylation under the high DOC concentration and high DOM $SUVA_{254}$ (Graham et al., 2013). Sulfate was not correlated to $RMP_{matrix}$ (Fig. S9d; $R^2 = 0.026$, $p = 0.051$). We infer that in this system and during the duration of the experiments, the DOM $SUVA_{254}$ is a more important variable than sulfide for controlling $Hg(II)_i$ bioavailability. This is highlighted by the similarity in $RMP_{matrix}$ of 2A-N pore water and F1 HPOA DOM, which were collected from proximal locations, albeit several years apart, and have similar DOM concentrations and $SUVA_{254}$ content, but very different sulfide concentrations (Fig. 2, S9).

The $Hg(II)_i$-cysteine solution yielded very low net MeHg formation across all six study sites (Fig. 1c, S8) despite having thiol concentration equimolar to the F1 HPOA solution, which is inconsistent with previous pure culture laboratory studies (Graham et al., 2012; Schaefer et al., 2011; Schaefer & Morel, 2009). This is particularly striking considering that cysteine levels in the environment are far lower than those used in this study (J. Zhang et al., 2004). This may be

298 explained by cysteine's lack of aromaticity needed to sterically inhibit nano-particulate β-HgS
299 growth (Gerbig et al., 2011; Poulin, Gerbig, et al., 2017; T. Zhang et al., 2012), or the rapid
300 degradation of cysteine under environmental conditions (Chu et al., 2016) that allows the
301 $^{201}Hg(II)_i$ tracer to sorb to the peat, thus diminishing its bioavailability. Regardless of the
302 mechanism, the findings support that cysteine-complexed $Hg(II)_i$ is unlikely to be
303 environmentally relevant for MeHg formation. In total, the results are in general concurrence
304 with laboratory studies demonstrating that aromatic, thiol-rich DOM plays a key role in
305 promoting $Hg(II)_i$ bioavailability (Graham et al., 2013), with the notable disagreement that
306 cysteine did not promote $Hg(II)_i$ bioavailability in nature.
307
308 **Microbial controls on $Hg(II)_i$ methylation**: The source of the peat cores also had a significant
309 effect on net $Me^{201}Hg$ production. As the filtered pore water matrices used for equilibration
310 controlled the bioavailability of the $^{201}Hg(II)_i$ tracer but contained no microbes, the influence of
311 the peat cores on net $Me^{201}Hg$ production reflected the Hg-methylation capacity of the microbial
312 community in the peat. The net $Me^{201}Hg$ production response to the peat cores was split in one
313 of two similar patterns depending on the pore water matrix used in the incubation, as described
314 above (Fig. 1c, S7). However, it was always very low in peat cores from sites with high
315 sulfate/sulfide (2A-N and 2A-A) and increased in peat cores from sites with low to non-
316 detectable sulfate/sulfide.
317 The relative methylation potential of the peat cores ($RMP_{peat}$) was quantified to identify
318 the relationship between the Hg-methylation capacity of the microbes and the abundance of the
319 *hgcA* gene. $RMP_{peat}$ was calculated by grouping all incubation assays by the pore water matrix

and normalizing net $Me^{201}Hg$ production to the highest level of $Me^{201}Hg$ produced within that group (Fig. S4). As observed with the raw net $Me^{201}Hg$ production data (Fig. S7), the $RMP_{peat}$ was lowest in peat cores from high sulfate sites (Site 2A-N, 2A-A) and increased systematically in cores with decreasing sulfate (Fig. S10). Eighty-seven unique *hgcA* genes across the six sites were identified using shotgun metagenomic sequencing of the peat cores (Tables S3-S5; additional details in Supporting Information). Normalized *hgcA* abundance correlated significantly and positively with $RMP_{peat}$ (adjusted $R^2 = 0.494$; $p < 0.0001$; Fig. 3a) due to an increase in *hgcA* abundance from sites with high sulfate to low sulfate (Fig. 3b). Previous attempts to correlate *hgcA* abundance to MeHg levels have met with mixed results (Bae et al., 2019; Bravo et al., 2016; Christensen et al., 2019; Liu et al., 2018; Millera Ferriz et al., 2021; Roth et al., 2021; Tada et al., 2020), possibly due to changes in $Hg(II)_i$ bioavailability or methodological constraints of qPCR-based *hgcA* quantification (McDaniel et al., 2020). Other studies suggest additional genes may confer MeHg production (Bowman et al., 2020; Munson et al., 2018). However, the correlation between *hgcA* gene abundance and the microbial Hg-methylation capacity suggests that *hgcA* is the dominant MeHg formation pathway in Everglades peat. Recent work showed decreases in *hgcA* alpha diversity to coincide with decreases in MeHg production thought to be independent of changes in $Hg(II)_i$ bioavailability (Jones et al., 2020). This may have reflected an overall decrease in *hgcA* abundance, as we also observed an increase in *hgcA* richness and evenness coincident with an increase in *hgcA* abundance and Hg-methylation capacity (Fig. S11). Transcription of *hgcA*, while thought to be constitutive based on experiments in culture (Gilmour et al., 2011; Goñi-Urriza et al., 2015), varies between different organisms in the environment (Capo, Broman, et al., 2022; McDaniel et al., 2020). Overall trends in *hgcA* gene abundance vs. expression were consistent in brackish waters (Capo, Feng, et

al., 2022), but exhibited divergent trends in sediments from the same site (Capo, Broman, et al., 2022). Collectively, this shows that the controls on *hgcA* gene expression are not well understood. Additionally, the relationship between *hgcA* expression and MeHg production by individual cells is unclear. However, the correlation observed between *hgcA* and $RMP_{peat}$ suggests that in this ecosystem at least, the *hgcA* abundance, independent of *hgcA* transcription or metabolic activity of the Hg-methylators, is sufficient to identify the Hg-methylation capacity of the microbial community.

Next, the community composition and metabolic potential of the microbes with *hgcA* (hgcA+) were evaluated to establish potential linkages between biogeochemical processes and MeHg formation (Table S6). Details of the metabolic analyses are provided in the Supporting Information. The trends in the beta diversity of *hgcA* are not aligned with the trends in the peat core $RMP_{peat}$ or sulfate levels (Fig. 3c). Methanogenic archaea-associated *hgcA* genes accounted for the largest portion of *hgcA* abundance (37% to 55% of the total *hgcA* coverage; Fig. 3b, S12, S13). These *hgcA* sequences were exclusively associated with predicted hydrogenotrophic or methylotrophic methanogens, but not acetoclastic methanogens, which is consistent with previous work (Gilmour et al., 2018) (Fig. 3d). Methanogen-associated *mcrA* genes increased in abundance across the sulfate gradient (Fig. S14a). A comparison of methanogen-associated *hgcA* and *mcrA* abundances indicates that 50-100% of methanogens across the sulfate gradient carried *hgcA* (Fig. 3b, S14a). The remainder of the *hgcA* sequences were from a diverse group of hgcA+ bacteria, including Chloroflexi, Aminicenantes, Spirochaetes, and non-SRB Syntrophobacterales, among other rarer groups (Table S5). Metabolic pathway analysis of reconstructed hgcA+ genomes from Chloroflexi, Aminicenantes, and Syntrophobacterales and comparison of unbinned *hgcA* to closely related genomes confirmed that all classified non-methanogen-

associated hgcA+ microbes in these peat cores are fermentative (Fig. 3d). Several *hgcA* genes were highly divergent from the *hgcA* sequences in the reference database, resulting in 0-5% of the *hgcA* genes (by abundance) being unclassified with no information on the metabolic potential. Importantly, none of the *hgcA* sequences were expected to be associated with SRB (Fig. 3d). This is not due to a lack of SRBs, as SRBs accounted for up to 4.5 or 7.5% (depending on the marker used) of the microbial population, increasing in abundance across the sulfate gradient (Fig. S14b). This surprising finding is discussed more below. Although subtle differences in the taxonomic affiliation of hgcA+ community members were observed across the six sites, the relative contribution of organisms from different levels of the microbial food web to the *hgcA* pool do not differ substantially with respect to sulfate levels (Fig. S13, 3d). Thus, we hypothesize that the metabolic pathways directly contributing to MeHg production are likely consistent across the sulfate gradient. This consistency and the linear relationship between $RMP_{peat}$ and overall *hgcA* abundance (Fig. 3a) suggest that the observed differences in the Hg-methylation capacity are governed by abundance of Hg-methylators rather than their metabolic activity.

While recent studies have shown SRBs to account for a small percentage of the microbial community even under sulfidic conditions (Capo, Broman, et al., 2022; Jones et al., 2019, 2020; Peterson et al., 2020), including within the greater Everglades ecosystem (Bae et al., 2014), none of these have found no SRB-associated *hgcA* sequences. Molybdate inhibition experiments have shown the importance of sulfate reduction for MeHg production in Everglades peat, particularly in the high sulfide sites (Bae et al., 2014; Gilmour et al., 1998). Together, this suggests that SRBs play some role in MeHg production in the peat that is not represented by the abundance of SRB-associated *hgcA* genes. One possibility is that rare *hgcA*-carrying SRBs, undetected due to

insufficient sequencing depth, controlled MeHg formation; however, this is unlikely given the complete absence of SRB-associated *hgcA* sequences and the close linear relationship between *hgcA* and MeHg production capacity (Fig. 3a). Alternatively, SRBs could indirectly control MeHg formation by controlling carbon and energy flow, both above (fermentation) and below (methanogenesis), through the anaerobic microbial food web, thus influencing the metabolic activity of hgcA+ organisms in the community. For example, under anoxic conditions, fermentative organisms break down and convert large organic molecules into smaller carbon compounds, but they rely on syntrophs or respiratory organisms to consume these products (Fig. 3d) (Arndt et al., 2013). SRBs can oxidize smaller organic molecules either by reducing sulfate or in syntrophy with methanogens, where they ferment volatile fatty acids (e.g., propionate, butyrate) to methanogenic substrates (acetate, $CO_2$, and hydrogen) (Sieber et al., 2012). The parallel increase in *mcrA* and *dsrAD* with decreasing sulfide levels may indicate increasing levels of SRB-methanogenic syntrophy (Fig. S14). These syntrophic interactions are known to enhance MeHg formation (Yu et al., 2018), and given the high *hgcA* abundance within the methanogenic community, may contribute to the observed increase in Hg-methylation capacity (Fig. S10). If *hgcA*-containing methanogens are reliant on SRB through syntrophy, this could explain the inhibition of MeHg formation by molybdate as well (Bae et al., 2014; Cleckner et al., 1999; Gilmour et al., 1998; Newport & Nedwell, 1988). Overall, we hypothesize that terminal respiration is dominated by sulfate reduction and hydrogenotrophic methanogenesis at sulfate-enriched sites, whereas low sulfate sites exhibit greater fermentation of small organic acids by SRB coupled syntrophically to hydrogenotrophic methanogenesis and acetate consumption by acetoclastic methanogens.

**MeHg production and accumulation:** A major knowledge gap in the field is whether $Hg(II)_i$ bioavailability or Hg-methylation capacity is the rate-limiting step for MeHg production in environmental systems. By isolating these two effects, we were able to compare them to each other and to the production of MeHg. There was no correlation between $Hg(II)_i$ bioavailability ($RMP_{matrix}$) vs. Hg-methylation capacity ($RMP_{peat}$; Fig. 4), suggesting that the ability of microbial communities to methylate Hg was not linked to how much bioavailable Hg was present. This supports the hypothesis that MeHg production is not the "native function" of *hgcA*, as has been proposed in previous work (Parks et al., 2013; Smith et al., 2015). We also compared how each factor influenced MeHg production under *in situ* conditions, termed "native MeHg production". Neither factor was solely limiting for native MeHg production; rather, a synergy of the two factors was required. Native MeHg production was only high at sites where both the pore water $RMP_{matrix}$ and the microbial community $RMP_{peat}$ were high (Fig. 4). For example, peat from sites 3A-O and 3A-N had similar hgcA+ microbial communities (Fig. 3b,c) that also corresponded to nearly identical $RMP_{peat}$ values (Fig. 3a). However, native MeHg production at site 3A-O was much higher due to higher $RMP_{matrix}$ values, which are linked to the higher DOM $SUVA_{254}$ promoting $Hg(II)_i$ bioavailability (Fig. 4). Conversely, the pore water $RMP_{matrix}$ at site 2A-N was similar to that at site 3A-O, but the low $RMP_{peat}$ at 2A-N was responsible for the very low native MeHg production (Fig. 4). This synergistic effect is consistent with work in brackish marine waters that showed predicted concentrations of $Hg(II)_i$-sulfide complexes and gene abundance or expression of *hgcA* collectively correlated with MeHg production potential (Capo, Feng, et al., 2022). Together, these data suggest that $Hg(II)_i$ bioavailability and the Hg-methylation capacity

of the microbial community both control MeHg formation under environmental conditions and that either of them can limit MeHg production (Fig. 5).

Another major knowledge gap is how MeHg production and the factors that govern it relate to ambient MeHg pools in sediment and porewater which have accumulated over time. In this study, MeHg concentrations in the peat (Fig. 1a) and porewater (Fig. 1b) increased systematically with decreasing sulfate. However, the pattern in $Me^{201}Hg$ formation under native conditions was much different, showing high MeHg formation rates at 3A-O and LOX8, but low at the other four sites (Fig. 1c). Additionally, we observed MeHg production up to 3.4% of the tracer under ambient conditions at 3A-O but the %MeHg values at this site are only 1.5%. These observations may be due, in part, to other biogeochemical processes influencing ambient MeHg levels that were not measured in this study. One likely possibility is that much of the ambient $Hg(II)_i$ is sorbed strongly to the peat and is not available for methylation, but it is unclear how this would change across the sulfate gradient. Another likely process is MeHg degradation, which does occur in Everglades peat (Gilmour et al., 1998; Marvin-DiPasquale & Oremland, 1998). The demethylation gene *merB* was detected at all sites and decreased in abundance as sulfate decreased, in opposition to the trend in *hgcA* (Fig. S15); however, demethylation occurs at a consistent rate across the sulfate gradient in Everglades peat (Marvin-DiPasquale & Oremland, 1998). Despite these other potential effects, calculated $RMP_{peat}$ values and ambient MeHg concentration in the peat were strongly and positively correlated (adjusted $R^2 = 0.885$; $p = 0.003$; Fig. S16a), while $RMP_{matrix}$ values were not correlated with ambient MeHg concentration in the peat (adjusted $R^2 = -0.250$; $p = 0.9759$; Fig. S16b). We propose that $RMP_{peat}$ represents the longer-term, site-specific MeHg production potential, whereas $RMP_{matrix}$ represents the potential shorter-term (seasonal) effects of aqueous ligands promoting $Hg(II)_i$ methylation.

**Role of sulfate in controlling MeHg production in the environment**: This study offers new insights into the long-standing hypothesis that sulfate and sulfide are the master variables controlling MeHg production and add complexity to the well-documented linkages between anthropogenic sulfate loading and MeHg production across the Everglades (Gilmour et al., 1998; Hurley et al., 1998; Orem et al., 2020) and other peatlands worldwide (Coleman Wasik et al., 2012, 2015; Mitchell et al., 2008; Poulin et al., 2019; Tjerngren et al., 2012). The current model is that at high sulfide concentrations, $Hg(II)_i$ bioavailability is drastically reduced, due to the formation of crystalline nano-particulate β-HgS of lower bioavailability (Gerbig et al., 2011; Gilmour et al., 2018; Poulin, Gerbig, et al., 2017; T. Zhang et al., 2012), while low sulfate concentrations result in lowered SRB activity, leading to reduced MeHg production. Collectively, this was used to explain the "Goldilocks curve" observed in the Everglades, where MeHg formation is maximized under intermediate sulfate/sulfide concentrations (Gilmour et al., 2007; Orem et al., 2020). However, we showed that the low MeHg production at high sulfate sites was due to reduced Hg-methylation capacity by the microbial community, despite the $Hg(II)_i$ bioavailability being high. For example, 2A-N pore water resulted in high MeHg production when paired with cores containing high *hgcA* abundance, but *hgcA* at 2A-N was low, resulting in low MeHg production under native conditions (Fig. 1c, 3b). At the low sulfate end of the gradient, microbial Hg-methylation capacity was highest, and the low bioavailability led to reduced MeHg production levels. For example, the peat cores from 3A-F produced high MeHg when provided with $^{201}Hg(II)_i$ equilibrated with pore water from 2A-N, LOX8, or F1 HPOA

DOM due to the high *hgcA* content, but the low bioavailability of $^{201}Hg(II)_i$ in 3A-F pore water drove low MeHg production under native conditions (Fig. 1c).

Thus, the influence of sulfate levels and SRB activity on Hg methylation in the Florida Everglades and similarly impacted wetlands is more complicated than previously described. Sulfate reduction exerts control on $Hg(II)_i$ bioavailability in a number of ways. While sulfide can precipitate $Hg(II)_{i\ (Poulin,\ Gerbig,\ et\ al.,\ 2017)}$, reducing its overall bioavailability, this is unlikely to be a dominant process in sites with high concentrations of aromatic DOM, given the high $Hg(II)_i$ bioavailability at the high sulfide sites (Fig. S8). On the other hand, moderate levels of sulfide, in the presence of aromatic DOM, can enhance methylation by promoting the formation of poorly crystalline nano-particulate β-HgS (Gerbig et al., 2011; Poulin, Gerbig, et al., 2017). Enhanced sulfate reduction can also promote peat degradation, enhancing the concentration of high-$SUVA_{254}$ DOM in wetland porewaters (Aiken et al., 2011; Luek et al., 2017), and increase the DOM $S_{Red}$ content via sulfurization (Poulin, Ryan, et al., 2017); both of these enhance the bioavailability of $Hg(II)_i$ to methylation (Graham et al., 2012, 2013, 2017; Jonsson et al., 2012; T. Zhang et al., 2012). The effects of sulfate loading on the Hg-methylating microbial community are less clear. Overall, both *hgcA* abundance and $RMP_{peat}$ decreased with higher overall sulfate concentrations (Fig. 3b, S10), consistent with the lack of hgcA+ SRBs and previous work showing a decrease in *hgcA* diversity and estimated Hg-methylation capacity with increased long-term sulfate loading (Jones et al., 2020). However, past work has clearly shown that SRB activity is important for MeHg production in the Everglades (Bae et al., 2014; Gilmour et al., 1998; Orem et al., 2020). Thus, we propose that SRBs influence MeHg production indirectly by stimulating overall microbial metabolism, possibly through consuming fermentation products (Arndt et al., 2013) and/or by stimulating methanogenic activity through

syntrophy (Sieber et al., 2012). Ultimately, functional assays and the deployment of next-generation physiology experiments (Hatzenpichler, 2020) are needed to further probe how the metabolic activity and interactions of the microbial community influence MeHg production.

## Conclusions and Environmental Implications

This study presents a dual examination of microbial and geochemical controls on MeHg production in natural peatlands, providing new insights into both the synergy between the hgcA+ fraction of the microbial community and geochemical controls on $Hg(II)_i$ bioavailability, and the direct and indirect roles of sulfate. The abundance of metabolically diverse populations with *hgcA* confer robust potential for Hg-methylation; when paired with geochemical conditions that promote $Hg(II)_i$ bioavailability, one can expect MeHg formation and a high potential for food web uptake and MeHg biomagnification to toxic levels. Given the widely recognized importance of sulfate on spatial and temporal trends in MeHg formation in wetlands globally (Coleman Wasik et al., 2012, 2015; Mitchell et al., 2008; Orem et al., 2020; Poulin et al., 2019; Tjerngren et al., 2012), a mechanistic understanding of the role of sulfate loading on MeHg production is critical. Peatland ecosystems are experiencing seasonal and long-term increases in sulfate levels in response to increased sulfate use in agricultural practices (Hinckley et al., 2020) and coastal wetland inundation with seawater sulfate (Chambers et al., 2019). The results here suggest that ecosystems with lower sulfate levels but high DOM concentration/$SUVA_{254}$ may be well-poised to form MeHg when sulfate levels increase due to the indirect effects of sulfate on $Hg(II)_i$ bioavailability. We postulate that the bioavailability of $Hg(II)_i$ in environments with lower DOC levels (e.g., marine waters) may be modulated by inorganic sulfide in addition to DOM. We still

have much to learn on how environmental conditions such as sulfate concentrations influence *hgcA* distribution and how interactions between different metabolic guilds influence overall MeHg formation rates. Notwithstanding, this study provides an important framework by which the individual factors that influence MeHg production can be isolated and highlights the need for more advanced methods to elucidate the mechanism by which these factors drive Hg methylation activity.

## Acknowledgements

This work was supported by the U.S. Geological Survey (USGS) Priority Ecosystems Science (PES) program (support to DPK and BAP). KDM and BDP were supported by a grant from the U.S. National Science Foundation (CBET-1935173). All mercury analyses were performed at the Upper Midwest Water Science Center in the Mercury Research Laboratory (U.S. Geological Survey, Madison, WI). Computational analyses were done on the Wisconsin Energy Institute computing cluster, which is funded by the Great Lakes Bioenergy Research Center as part of the U.S. Department of Energy Office of Science. Any use of trade, product, or firm names in this publication is for descriptive purposes only and does not imply endorsement by the U.S. Government. All authors declare no conflict of interest.

## Supplemental Tables

Supplemental tables are provided in separate Excel sheet with Supporting Information.

Table S1: GPS coordinates of field sampling sites.

Table S2: Data from Hg-methylation experiments.

Table S3: Metagenomic sequencing information.

Table S4: Statistics from metagenomic assemblies.

Table S5: *hgcA* gene information.

Table S6: Information on reconstructed hgcA+ genomic bins.

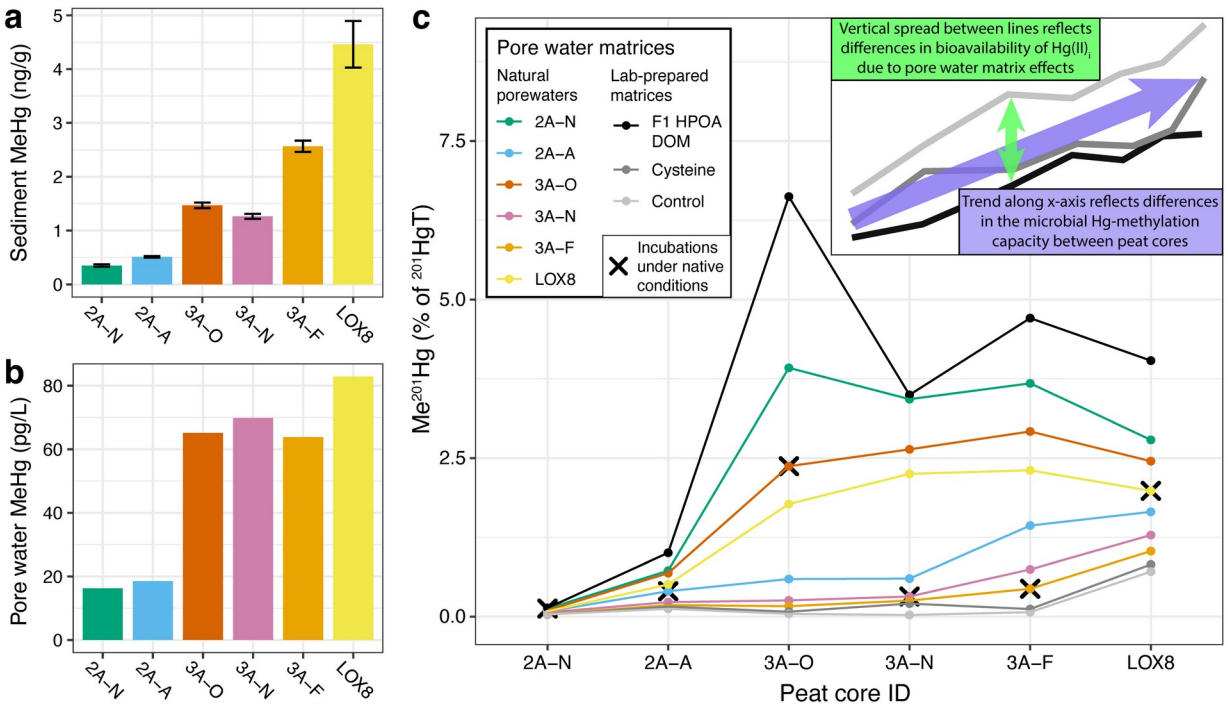


**Figure 1**. Ambient MeHg levels in (A) sediment and (B) pore water, and (C) summary of MeHg formation assay results. Sediment MeHg values represent the average ambient MeHg values across all 18 peat cores from each site. MeHg formation assay results present the mean of duplicate incubations with peat cores and pore waters from the same source. $Me^{201}Hg$ values are expressed as a percent of the measured $^{201}HgT$. Data points marked “X” identify incubations under “native” conditions, where the injected pore water matrices were from the same sites as the peat cores. The inset provides guides for the interpretations of x- and y-axis trends in plot C.

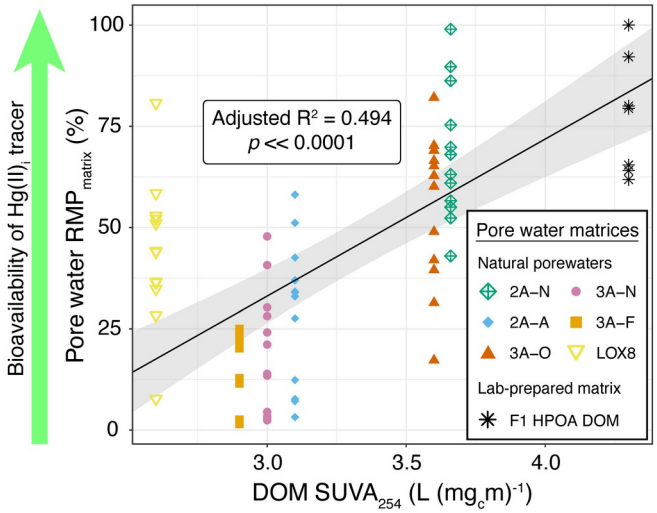


**Figure 2**. Linear correlation between the pore water relative methylation potential ($RMP_{matrix}$) and DOM $SUVA_{254}$ in the pore water matrices injected into peat cores. The black line represents the linear regression, and the gray shading corresponds to the 98% confidence intervals of the linear fit. The control and cysteine pore water matrices were not included because the solutions do not have $SUVA_{254}$ values. Some jitter was added to the x-axis to improve visibility of points that were stacked on top of each other, but all points of the same color have the same $SUVA_{254}$ values. One of the F1 HPOA DOM replicates always resulted in the highest $Me^{201}Hg$ production, so there are six points stacked at x = 4.3 L $(mg_cm)^{-1}$, y = 100%.

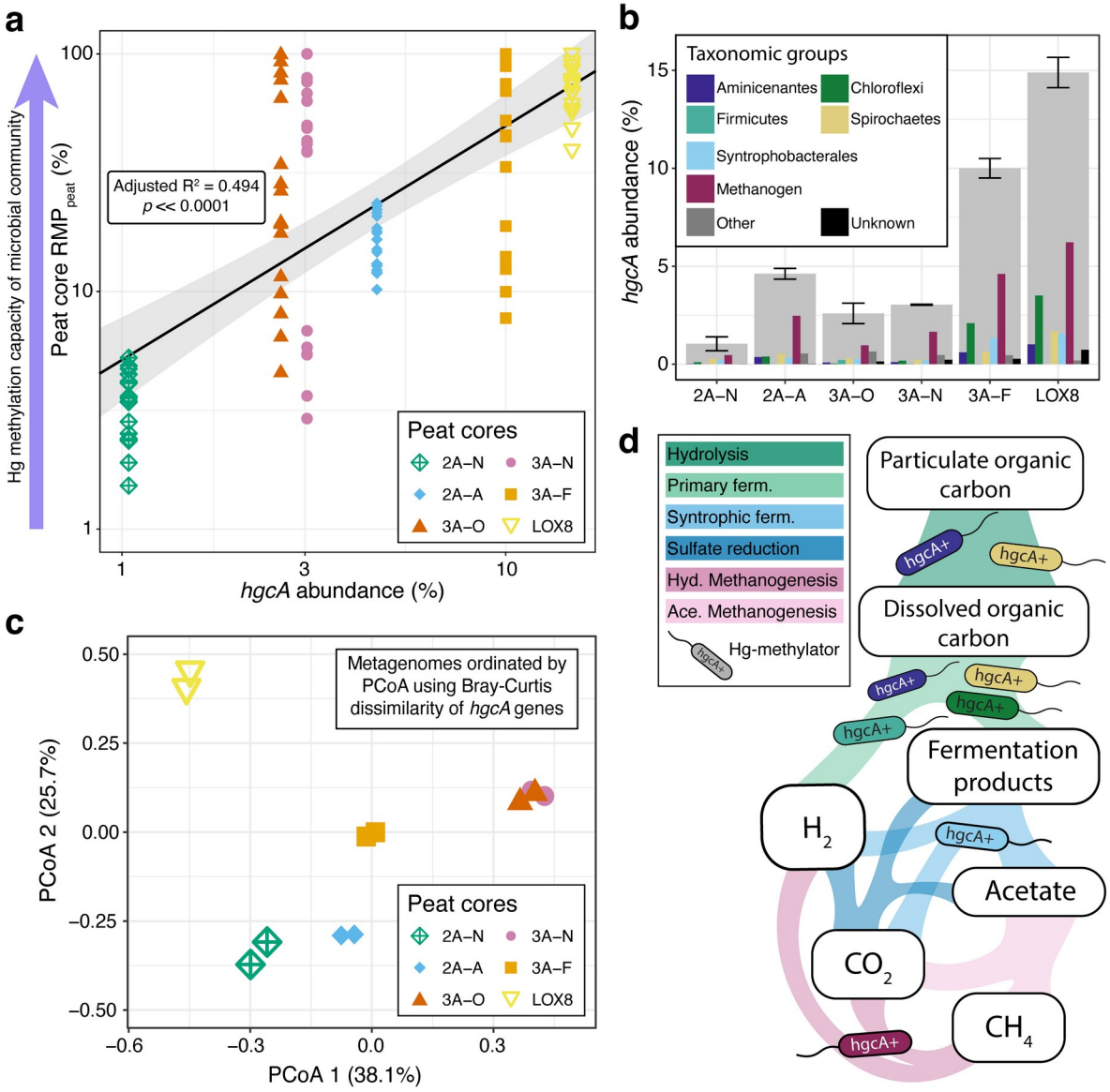


**Figure 3**. Characterization of the microbial community fraction with potential for Hg methylation. (A) The linear correlation between the peat core relative methylation potential ($RMP_{peat}$) and the normalized *hgcA* abundance at each site. Both variables were log-transformed before regression. The black line represents the linear regression, and the gray shading corresponds to the 98% confidence intervals of the linear fit. All points of the same color have the same *hgcA* abundance, but some jitter was added to the x-axis to improve readability. (B) Bar chart of normalized *hgcA* abundance, with the cumulative abundance of all *hgcA* sequences shown in gray bars and the abundance of individual taxonomic groups shown in colored bars. Abundance data are presented as the mean normalized abundance of *hgcA* in two duplicate metagenomes, with the errors bars on the cumulative abundance representing the standard error of duplicates. (C) Principal coordinate analysis (PCoA) of metagenomes based on the Bray-

Curtis dissimilarity of the *hgcA* population in each metagenome. (D) A conceptual model of the anaerobic microbial food web present across the sulfate gradient, with the microbes denoting levels at which organisms with *hgcA* were identified. Colors of microbes correspond to taxonomic classification in (B). Abbreviations: Ferm. = Fermentation; Hyd. = Hydrogenotrophic; Ace. = Acetoclastic.

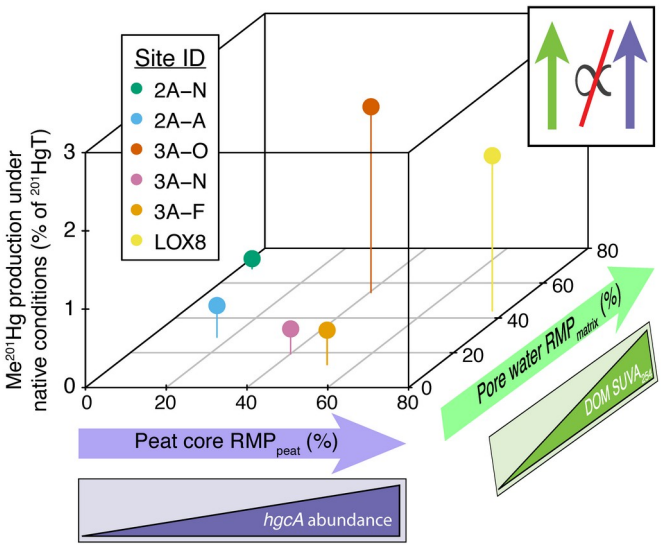


**Figure 4**. Effects of $Hg(II)_i$ bioavailability and Hg methylation capacity of microbial community on the production of MeHg under "native" conditions. Native MeHg production is based on MeHg formation assay results using peat cores injected with $^{201}Hg(II)_i$ equilibrated with pore water from the same site. Data are presented as the percent of $^{201}HgT$ measured as $Me^{201}Hg$. Environmental parameters that were observed to influence the bioavailability of $Hg(II)_i$ and the microbial methylation of $Hg(II)_i$ are shown below the respective axes. Inset shows there is no correlation between $RMP_{matrix}$ and $RMP_{peat}$ ($p$ = 0.32).

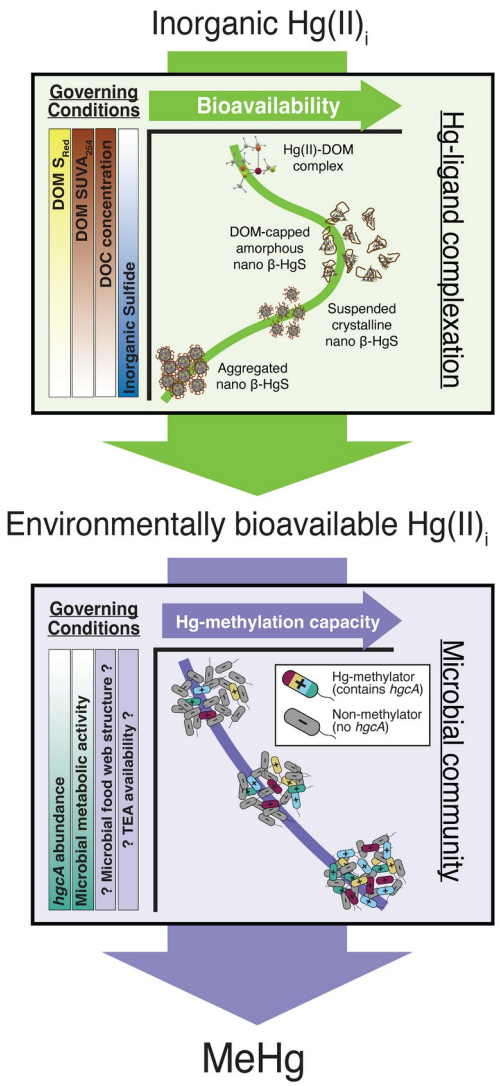


**Figure 5**. Conceptual model of MeHg production as a two-step process: first, the formation of bioavailable $Hg(II)_i$, followed by microbial methylation of bioavailable $Hg(II)_i$. Environmental MeHg formation is limited by both factors, which in turn have several environmental drivers. The roles of DOM quantity/ composition and sulfide in regulating bioavailable $Hg(II)_i$ in the environment is informed by results of this study and others on $Hg(II)_i$ complexation (Haitzer et al., 2002; Manceau et al., 2015), nano-particulate β-HgS formation (Gerbig et al., 2011; Poulin, Gerbig, et al., 2017) and $Hg(II)_i$ bioavailability to methylation (Graham et al., 2012, 2013, 2017; T. Zhang et al., 2012). The relationship between *hgcA* abundance and Hg-methylation capacity of a microbial community is informed by results of this study and others on *hgcA*-based Hg methylation (Gilmour et al., 2013; Parks et al., 2013) and Hg-methylation correlations with overall microbial activity (Guimarães et al., 2006). While many studies have identified Hg methylators across the anaerobic microbial food web (Gilmour et al., 2013; Gionfriddo et al., 2016; Jones et al., 2019; McDaniel et al., 2020; Peterson et al., 2020), it is

still unknown how the distribution of *hgcA* across these metabolic guilds or their response to changing terminal electron acceptors (TEA) influences MeHg production.

## References


Aiken, G. R., Gilmour, C. C., Krabbenhoft, D. P., & Orem, W. H. (2011). Dissolved organic matter in the Florida Everglades: Implications for ecosystem restoration. *Critical Reviews in Environmental Science and Technology*, *41*(S1), 217–248. https://doi.org/10.1080/10643389.2010.530934

Alneberg, J., Bjarnason, B. S., de Bruijn, I., Schirmer, M., Quick, J., Ijaz, U. Z., Lahti, L., Loman, N. J., Andersson, A. F., & Quince, C. (2014). Binning metagenomic contigs by coverage and composition. *Nature Methods*, *11*(11), 1144–1146. https://doi.org/10.1038/nmeth.3103

Arndt, S., Jørgensen, B. B., LaRowe, D. E., Middelburg, J. J., Pancost, R. D., & Regnier, P. (2013). Quantifying the degradation of organic matter in marine sediments: A review and synthesis. *Earth-Science Reviews*, *123*, 53–86. https://doi.org/10.1016/j.earscirev.2013.02.008

Bae, H.-S., Dierberg, F. E., & Ogram, A. (2014). Syntrophs dominate sequences associated with the mercury methylation-related gene *hgcA* in the Water Conservation Areas of the Florida Everglades. *Applied and Environmental Microbiology*, *80*(20), 6517–6526. https://doi.org/10.1128/AEM.01666-14

Bae, H.-S., Dierberg, F. E., & Ogram, A. (2019). Periphyton and flocculent materials are important ecological compartments supporting abundant and diverse mercury methylator assemblages in the Florida

Everglades. *Applied and Environmental Microbiology*, *85*(13). https://doi.org/10.1128/AEM.00156-19

Basso, D., Pesarin, F., Salmaso, L., & Solari, A. (2009). *Permutation tests for stochastic ordering and ANOVA: Theory and applications with R*. Springer.

Benoit, J. M., Gilmour, C. C., Mason, R. P., & Heyes, A. (1999). Sulfide controls on mercury speciation and bioavailability to methylating bacteria in sediment pore waters. *Environmental Science & Technology*, *33*(6), 951–957. https://doi.org/10.1021/es9808200

Bouchet, S., Goñi-Urriza, M., Monperrus, M., Guyoneaud, R., Fernandez, P., Heredia, C., Tessier, E., Gassie, C., Point, D., Guédron, S., Achá, D., & Amouroux, D. (2018). Linking microbial activities and low-molecular-weight thiols to Hg methylation in biofilms and periphyton from high-altitude tropical lakes in the Bolivian Altiplano. *Environmental Science & Technology*, *52*(17), 9758–9767. https://doi.org/10.1021/acs.est.8b01885

Bowman, K. L., Collins, R. E., Agather, A. M., Lamborg, C. H., Hammerschmidt, C. R., Kaul, D., Dupont, C. L., Christensen, G. A., & Elias, D. A. (2020). Distribution of mercury-cycling genes in the Arctic and equatorial Pacific Oceans and their relationship to mercury speciation. *Limnology and Oceanography*, *65*, S310–S320. https://doi.org/10.1002/lno.11310

Bravo, A. G., Loizeau, J.-L., Dranguet, P., Makri, S., Björn, E., Ungureanu, V. Gh., Slaveykova, V. I., & Cosio, C. (2016). Persistent Hg contamination and occurrence of Hg-methylating transcript (*hgcA*) downstream of a chlor-alkali plant in the Olt River (Romania). *Environmental Science and Pollution Research*, *23*(11), 10529–10541. https://doi.org/10.1007/s11356-015-5906-4

Capo, E., Broman, E., Bonaglia, S., Bravo, A. G., Bertilsson, S., Soerensen, A. L., Pinhassi, J., Lundin, D., Buck, M., Hall, P. O. J., Nascimento, F. J. A., & Björn, E. (2022). Oxygen-deficient water zones in the Baltic Sea promote uncharacterized Hg methylating microorganisms in underlying sediments. *Limnology and Oceanography*, *67*, 135–146. https://doi.org/10.1002/lno.11981

Capo, E., Feng, C., Bravo, A. G., Bertilsson, S., Soerensen, A. L., Pinhassi, J., Buck, M., Karlsson, C., Hawkes, J., & Björn, E. (2022). Expression levels of *hgcAB* genes and mercury availability jointly explain methylmercury formation in stratified brackish waters. *Environmental Science & Technology*, *56*(18), 13119–13130. https://doi.org/10.1021/acs.est.2c03784

Chambers, L. G., Steinmuller, H. E., & Breithaupt, J. L. (2019). Toward a mechanistic understanding of “peat collapse” and its potential contribution to coastal wetland loss. *Ecology*, *100*(7), e02720. https://doi.org/10.1002/ecy.2720

Chaumeil, P.-A., Mussig, A. J., Hugenholtz, P., & Parks, D. H. (2019). GTDB-Tk: A toolkit to classify genomes with the Genome Taxonomy Database. *Bioinformatics*, *36*(6), 1925–1927. https://doi.org/10.1093/bioinformatics/btz848

Christensen, G. A., Gionfriddo, C. M., King, A. J., Moberly, J. G., Miller, C. L., Somenahally, A. C., Callister, S. J., Brewer, H., Podar, M., Brown, S. D., Palumbo, A. V., Brandt, C. C., Wymore, A. M., Brooks, S. C., Hwang, C., Fields, M. W., Wall, J. D., Gilmour, C. C., & Elias, D. A. (2019). Determining the reliability of measuring mercury cycling gene abundance with correlations with mercury and methylmercury concentrations. *Environmental Science & Technology*, *53*(15), 8649–8663. https://doi.org/10.1021/acs.est.8b06389

Christensen, G. A., Somenahally, A. C., Moberly, J. G., Miller, C. M., King, A. J., Gilmour, C. C., Brown, S. D., Podar, M., Brandt, C. C., Brooks, S. C., Palumbo, A. V., Wall, J. D., & Elias, D. A. (2018). Carbon amendments alter microbial community structure and net mercury methylation potential in sediments. *Applied and Environmental Microbiology*, *84*(3), e01049-17. https://doi.org/10.1128/AEM.01049-17

Chu, C., Erickson, P. R., Lundeen, R. A., Stamatelatos, D., Alaimo, P. J., Latch, D. E., & McNeill, K. (2016). Photochemical and nonphotochemical transformations of cysteine with dissolved organic matter. *Environmental Science & Technology*, *50*(12), 6363–6373. https://doi.org/10.1021/acs.est.6b01291

Cleckner, L. B., Gilmour, C. C., Hurley, J. P., & Krabbenhoft, D. P. (1999). Mercury methylation in periphyton of the Florida Everglades. *Limnology and Oceanography*, *44*(7), 1815–1825. https://doi.org/10.4319/lo.1999.44.7.1815

Coleman Wasik, J. K., Engstrom, D. R., Mitchell, C. P. J., Swain, E. B., Monson, B. A., Balogh, S. J., Jeremiason, J. D., Branfireun, B. A., Kolka, R. K., & Almendinger, J. E. (2015). The effects of hydrologic fluctuation and sulfate regeneration on mercury cycling in an experimental peatland. *Journal of Geophysical Research: Biogeosciences*, *120*(9), 1697–1715. https://doi.org/10.1002/2015JG002993

Coleman Wasik, J. K., Mitchell, C. P. J., Engstrom, D. R., Swain, E. B., Monson, B. A., Balogh, S. J., Jeremiason, J. D., Branfireun, B. A., Eggert, S. L., Kolka, R. K., & Almendinger, J. E. (2012). Methylmercury declines in a boreal peatland when experimental sulfate deposition decreases. *Environmental Science & Technology*, *46*(12), 6663–6671. https://doi.org/10.1021/es300865f

Compeau, G. C., & Bartha, R. (1985). Sulfate-reducing bacteria: Principal methylators of mercury in anoxic estuarine sediment. *Applied and Environmental Microbiology*, *50*(2), 498–502.

DeWild, J. F., Olson, M. L., & Olund, S. D. (2002). *Determination of Methyl Mercury by Aqueous Phase Ethylation, Followed by Gas Chromatographic Separation with Cold Vapor Atomic Fluorescence Detection. Open-file Report* (No. 2001–445). U. S. Geological Survey.

737 Eren, A. M., Esen, Ö. C., Quince, C., Vineis, J. H., Morrison, H. G., Sogin, M. L.,
738 & Delmont, T. O. (2015). Anvi'o: An advanced analysis and
739 visualization platform for 'omics data. *PeerJ*, *3*, 1–29.
740 https://doi.org/10.7717/peerj.1319
741 Fu, L., Niu, B., Zhu, Z., Wu, S., & Li, W. (2012). CD-HIT: Accelerated for
742 clustering the next-generation sequencing data. *Bioinformatics*,
743 *28*(23), 3150–3152. https://doi.org/10.1093/bioinformatics/bts565
744 Gascón Díez, E., Loizeau, J.-L., Cosio, C., Bouchet, S., Adatte, T., Amouroux,
745 D., & Bravo, A. G. (2016). Role of settling particles on mercury
746 methylation in the oxic water column of freshwater systems.
747 *Environmental Science & Technology*, *50*(21), 11672–11679.
748 https://doi.org/10.1021/acs.est.6b03260
749 Gerbig, C. A., Kim, C. S., Stegemeier, J. P., Ryan, J. N., & Aiken, G. R. (2011).
750 Formation of nanocolloidal metacinnabar in mercury-DOM-sulfide
751 Systems. *Environmental Science & Technology*, *45*(21), 9180–9187.
752 https://doi.org/10.1021/es201837h
753 Gilmour, C. C., Bullock, A. L., McBurney, A., Podar, M., & Elias, D. A. (2018).
754 Robust mercury methylation across diverse methanogenic *Archaea*.
755 *MBio*, *9*(2). https://doi.org/10.1128/mBio.02403-17
756 Gilmour, C. C., Elias, D. A., Kucken, A. M., Brown, S. D., Palumbo, A. V.,
757 Schadt, C. W., & Wall, J. D. (2011). Sulfate-reducing bacterium
758 *Desulfovibrio desulfuricans* ND132 as a model for understanding
759 bacterial mercury methylation. *Applied and Environmental*

*Microbiology*, *77*(12), 3938–3951. https://doi.org/10.1128/AEM.02993-10

Gilmour, C. C., Henry, E. A., & Mitchell, R. (1992). Sulfate stimulation of mercury methylation in freshwater sediments. *Environmental Science & Technology*, *26*(11), 2281–2287. https://doi.org/10.1021/es00035a029

Gilmour, C. C., Krabbenhoft, D., Orem, W. H., Aiken, G., & Roden, E. (2007). *Appendix 3B-2: Status Report on ACME Studies on the Control of Mercury Methylation and Bioaccumulation in the Everglades*. 39.

Gilmour, C. C., Podar, M., Bullock, A. L., Graham, A. M., Brown, S. D., Somenahally, A. C., Johs, A., Hurt, R. A., Bailey, K. L., & Elias, D. A. (2013). Mercury methylation by novel microorganisms from new environments. *Environmental Science & Technology*, *47*(20), 11810–11820. https://doi.org/10.1021/es403075t

Gilmour, C. C., Riedel, G. S., Ederington, M. C., Bell, J. T., Benoit, J. M., Gill, G. A., & Stordal, M. C. (1998). Methylmercury concentrations and production rates across a trophic gradient in the northern Everglades. *Biogeochemistry*, *40*, 327–345.

Gionfriddo, C. M., Capo, E., Peterson, B. D., Heyu, L., Jones, D. S., Bravo, A. G., Bertilsson, S., Moreau, J. W., McMahon, K. D., Elias, D. A., & Gilmour, C. C. (2021). *Hg-MATE-Db.v1.01142021*. https://doi.org/10.25573/serc.13105370.v1

Gionfriddo, C. M., Tate, M. T., Wick, R. R., Schultz, M. B., Zemla, A., Thelen, M. P., Schofield, R., Krabbenhoft, D. P., Holt, K. E., & Moreau, J. W. (2016). Microbial mercury methylation in Antarctic sea ice. *Nature Microbiology*, *1*(10). https://doi.org/10.1038/nmicrobiol.2016.127

Gionfriddo, C. M., Wymore, A. M., Jones, D. S., Wilpiszeski, R. L., Lynes, M. M., Christensen, G. A., Soren, A., Gilmour, C. C., Podar, M., & Elias, D. A. (2020). An improved *hgcAB* primer set and direct high-throughput sequencing expand Hg-methylator diversity in nature. *Frontiers in Microbiology*, *11*, 1–23. https://doi.org/10.3389/fmicb.2020.541554

Goñi-Urriza, M., Corsellis, Y., Lanceleur, L., Tessier, E., Gury, J., Monperrus, M., & Guyoneaud, R. (2015). Relationships between bacterial energetic metabolism, mercury methylation potential, and *hgcA*/*hgcB* gene expression in *Desulfovibrio dechloroacetivorans* BerOc1. *Environmental Science and Pollution Research*, *22*(18), 13764–13771. https://doi.org/10.1007/s11356-015-4273-5

Graham, A. M., Aiken, G. R., & Gilmour, C. C. (2012). Dissolved organic matter enhances microbial mercury methylation under sulfidic conditions. *Environmental Science & Technology*, *46*(5), 2715–2723. https://doi.org/10.1021/es203658f

Graham, A. M., Aiken, G. R., & Gilmour, C. C. (2013). Effect of dissolved organic matter source and character on microbial Hg methylation in Hg–S–DOM solutions. *Environmental Science & Technology*, *47*(11), 5746–5754. https://doi.org/10.1021/es400414a

Graham, A. M., Cameron-Burr, K. T., Hajic, H. A., Lee, C., Msekela, D., & Gilmour, C. C. (2017). Sulfurization of dissolved organic matter increases Hg–sulfide–dissolved organic matter bioavailability to a Hg-methylating bacterium. *Environmental Science & Technology*, *51*(16), 9080–9088. https://doi.org/10.1021/acs.est.7b02781

Guimarães, J. R. D., Mauro, J. B. N., Meili, M., Sundbom, M., Haglund, A. L., Coelho-Souza, S. A., & Hylander, L. D. (2006). Simultaneous radioassays of bacterial production and mercury methylation in the periphyton of a tropical and a temperate wetland. *Journal of Environmental Management*, *81*(2), 95–100. https://doi.org/10.1016/j.jenvman.2005.09.023

Haitzer, M., Aiken, G. R., & Ryan, J. N. (2002). Binding of mercury(II) to dissolved organic matter: The role of the mercury-to-DOM concentration ratio. *Environmental Science & Technology*, *36*(16), 3564–3570. https://doi.org/10.1021/es025699i

Hatzenpichler, R. (2020). Next-generation physiology approaches to study microbiome function at single cell level. *Nature Reviews Microbiology*, *18*, 16. https://doi.org/10.1038/ s41579-020-0323-1

Hinckley, E.-L. S., Crawford, J. T., Fakhraei, H., & Driscoll, C. T. (2020). A shift in sulfur-cycle manipulation from atmospheric emissions to agricultural additions. *Nature Geoscience*, *13*(9), 597–604. https://doi.org/10.1038/ s41561-020-0620-3

827 Hintelmann, H., & Evans, R. D. (1997). Application of stable isotopes in
828 environmental tracer studies—Measurement of monomethylmercury
829 ($CH_3Hg^+$) by isotope dilution ICP-MS and detection of species
830 transformation. *Fresenius' Journal of Analytical Chemistry*, *358*(3), 378–
831 385. https://doi.org/10.1007/s002160050433
832 Hsu-Kim, H., Kucharzyk, K. H., Zhang, T., & Deshusses, M. A. (2013).
833 Mechanisms regulating mercury bioavailability for methylating
834 microorganisms in the aquatic environment: A critical review.
835 *Environmental Science & Technology*, *47*(6), 2441–2456.
836 https://doi.org/10.1021/es304370g
837 Hurley, J. P., Krabbenhoft, D. P., Cleckner, L. B., Olson, M. L., Aiken, G. R., &
838 Jr, P. S. R. (1998). System controls on the aqueous distribution of
839 mercury in the northern Florida Everglades. *Biogeochemistry*, *40*, 293–
840 310.
841 Hyatt, D., Chen, G.-L., LoCascio, P. F., Land, M. L., Larimer, F. W., & Hauser,
842 L. J. (2010). Prodigal: Prokaryotic gene recognition and translation
843 initiation site identification. *BMC Bioinformatics*, *11*(119).
844 https://doi.org/10.1186/1471-2105-11-119
845 Janssen, S. E., Schaefer, J. K., Barkay, T., & Reinfelder, J. R. (2016).
846 Fractionation of mercury stable isotopes during microbial
847 methylmercury production by iron- and sulfate-reducing bacteria.
848 *Environmental Science & Technology*, *50*(15), 8077–8083.
849 https://doi.org/10.1021/acs.est.6b00854

Jones, D. S., Johnson, N. W., Mitchell, C. P. J., Walker, G. M., Bailey, J. V., Pastor, J., & Swain, E. B. (2020). Diverse communities of *hgcAB*$^{+}$ microorganisms methylate mercury in freshwater sediments subjected to experimental sulfate loading. *Environmental Science & Technology*, *54*, 14265−14274. https://doi.org/10.1021/acs.est.0c02513

Jones, D. S., Walker, G. M., Johnson, N. W., Mitchell, C. P. J., Coleman Wasik, J. K., & Bailey, J. V. (2019). Molecular evidence for novel mercury methylating microorganisms in sulfate-impacted lakes. *The ISME Journal*, *13*, 1659–1675. https://doi.org/10.1038/s41396-019-0376-1

Jonsson, S., Skyllberg, U., Nilsson, M. B., Lundberg, E., Andersson, A., & Björn, E. (2014). Differentiated availability of geochemical mercury pools controls methylmercury levels in estuarine sediment and biota. *Nature Communications*, *5*, 4624. https://doi.org/10.1038/ncomms5624

Jonsson, S., Skyllberg, U., Nilsson, M. B., Westlund, P.-O., Shchukarev, A., Lundberg, E., & Björn, E. (2012). Mercury methylation rates for geochemically relevant $Hg^{II}$ species in sediments. *Environmental Science & Technology*, *46*(21), 11653–11659. https://doi.org/10.1021/es3015327

Krabbenhoft, D. P., Hurley, J. P., Olson, M. L., & Cleckner, L. B. (1998). Diel variability of mercury phase and species distributions in the Florida Everglades. *Biogeochemistry*, *40*, 311–325.

Kucharzyk, K. H., Deshusses, M. A., Porter, K. A., & Hsu-Kim, H. (2015). Relative contributions of mercury bioavailability and microbial growth

rate on net methylmercury production by anaerobic mixed cultures. *Environmental Science: Processes & Impacts*, *17*(9), 1568–1577. https://doi.org/10.1039/C5EM00174A

Lever, M. A., Torti, A., Eickenbusch, P., Michaud, A. B., Å antl-Temkiv, T., & JÃ¸rgensen, B. B. (2015). A modular method for the extraction of DNA and RNA, and the separation of DNA pools from diverse environmental sample types. *Frontiers in Microbiology*, *6*. https://doi.org/10.3389/fmicb.2015.00476

Li, D., Liu, C.-M., Luo, R., Sadakane, K., & Lam, T.-W. (2015). MEGAHIT: An ultra-fast single-node solution for large and complex metagenomics assembly via succinct de Bruijn graph. *Bioinformatics*, *31*(10), 1674–1676. https://doi.org/10.1093/bioinformatics/btv033

Liu, Y.-R., Johs, A., Bi, L., Lu, X., Hu, H.-W., Sun, D., He, J.-Z., & Gu, B. (2018). Unraveling microbial communities associated with methylmercury production in paddy soils. *Environmental Science & Technology*, *52*(22), 13110–13118. https://doi.org/10.1021/acs.est.8b03052

Luek, J. L., Thompson, K. E., Larsen, R. K., Heyes, A., & Gonsior, M. (2017). Sulfate reduction in sediments produces high levels of chromophoric dissolved organic matter. *Scientific Reports*. https://doi.org/10.1038/s41598-017-09223-z

Manceau, A., Lemouchi, C., Rovezzi, M., Lanson, M., Glatzel, P., Nagy, K. L., Gautier-Luneau, I., Joly, Y., & Enescu, M. (2015). Structure, bonding, and stability of mercury complexes with thiolate and thioether ligands

from high-resolution XANES spectroscopy and first-principles calculations. *Inorganic Chemistry*, *54*(24), 11776–11791. https://doi.org/10.1021/acs.inorgchem.5b01932

Marvin-DiPasquale, M. C., & Oremland, R. S. (1998). Bacterial methylmercury degradation in Florida Everglades peat sediment. *Environmental Science & Technology*, *32*(17), 2556–2563. https://doi.org/10.1021/es971099l

McDaniel, E. A., Peterson, B. D., Stevens, S. L. R., Tran, P. Q., Anantharaman, K., & McMahon, K. D. (2020). Expanded phylogenetic diversity and metabolic flexibility of mercury-methylating microorganisms. *MSystems*, *5*(4). https://doi.org/10.1128/mSystems.00299-20

Millera Ferriz, L., Ponton, D. E., Storck, V., Leclerc, M., Bilodeau, F., Walsh, D. A., & Amyot, M. (2021). Role of organic matter and microbial communities in mercury retention and methylation in sediments near run-of-river hydroelectric dams. *Science of The Total Environment*, *774*. https://doi.org/10.1016/j.scitotenv.2021.145686

Mitchell, C. P. J., Branfireun, B. A., & Kolka, R. K. (2008). Assessing sulfate and carbon controls on net methylmercury production in peatlands: An *in situ* mesocosm approach. *Applied Geochemistry*, *23*(3), 503–518. https://doi.org/10.1016/j.apgeochem.2007.12.020

Moreau, J. W., Gionfriddo, C. M., Krabbenhoft, D. P., Ogorek, J. M., DeWild, J. F., Aiken, G. R., & Roden, E. E. (2015). The effect of natural organic matter on mercury methylation by *Desulfobulbus propionicus* 1pr3.

*Frontiers in Microbiology*, *6*, 1389. https://doi.org/10.3389/fmicb.2015.01389

Munson, K. M., Lamborg, C. H., Boiteau, R. M., & Saito, M. A. (2018). Dynamic mercury methylation and demethylation in oligotrophic marine water. *Biogeosciences*, *15*, 6451–6460. https://doi.org/10.5194/bg-2018-173

Newport, P. J., & Nedwell, D. B. (1988). The mechanisms of inhibition of *Desulfovibrio* and *Desulfotomaculum* species by selenate and molybdate. *Journal of Applied Bacteriology*, *65*(5), 419–423. https://doi.org/10.1111/j.1365-2672.1988.tb01911.x

Nurk, S., Meleshko, D., Korobeynikov, A., & Pevzner, P. A. (2017). metaSPAdes: A new versatile metagenomic assembler. *Genome Research*, *27*(5), 824–834. https://doi.org/10.1101/gr.213959.116

Olund, S. D., DeWild, J. F., Olson, M. L., & Tate, M. T. (2004). Methods for the preparation and analysis of solids and suspended solids for total mercury. In *U.S. Geological Survey Techniques of Water-Resources Investigations, Book 5, Chapter A8*.

Orem, W. H., Gilmour, C., Axelrad, D., Krabbenhoft, D., Scheidt, D., Kalla, P., McCormick, P., Gabriel, M., & Aiken, G. (2011). Sulfur in the south Florida ecosystem: Distribution, sources, biogeochemistry, impacts, and management for restoration. *Critical Reviews in Environmental Science and Technology*, *41*(sup1), 249–288. https://doi.org/10.1080/10643389.2010.531201

Orem, W. H., Krabbenhoft, D. P., Poulin, B. A., & Aiken, G. R. (2020). Chapter 2: Sulfur contamination in the Everglades, a major control on mercury methylation. In *Mercury and the Everglades. A Synthesis and Model for Complex Ecosystem Restoration: Volume II – Aquatic Mercury Cycling and Bioaccumulation in the Everglades: Vol. II*. Springer International Publishing. https://doi.org/10.1007/978-3-030-32057-7

Parks, J. M., Johs, A., Podar, M., Bridou, R., Hurt, R. A., Smith, S. D., Tomanicek, S. J., Qian, Y., Brown, S. D., Brandt, C. C., Palumbo, A. V., Smith, J. C., Wall, J. D., Elias, D. A., & Liang, L. (2013). The genetic basis for bacterial mercury methylation. *Science*, *339*(6125), 1332–1335. https://doi.org/10.1126/science.1230667

Peterson, B. D., McDaniel, E. A., Schmidt, A. G., Lepak, R. F., Janssen, S. E., Tran, P. Q., Marick, R. A., Ogorek, J. M., DeWild, J. F., Krabbenhoft, D. P., & McMahon, K. D. (2020). Mercury methylation genes identified across diverse anaerobic microbial guilds in a eutrophic sulfate-enriched lake. *Environmental Science & Technology*, *54*, 15840–15851. https://doi.org/10.1021/acs.est.0c05435

Podar, M., Gilmour, C. C., Brandt, C. C., Soren, A., Brown, S. D., Crable, B. R., Palumbo, A. V., Somenahally, A. C., & Elias, D. A. (2015). Global prevalence and distribution of genes and microorganisms involved in mercury methylation. *Science Advances*, *1*(9). https://doi.org/10.1126/sciadv.1500675

963 Poulin, B. A., Gerbig, C. A., Kim, C. S., Stegemeier, J. P., Ryan, J. N., & Aiken,
964 G. R. (2017). Effects of sulfide concentration and dissolved organic
965 matter characteristics on the structure of nanocolloidal metacinnabar.
966 *Environmental Science & Technology*, *51*(22), 13133–13142.
967 https://doi.org/10.1021/acs.est.7b02687
968 Poulin, B. A., Ryan, J. N., Nagy, K. L., Stubbins, A., Dittmar, T., Orem, W. H.,
969 Krabbenhoft, D. P., & Aiken, G. R. (2017). Spatial dependence of
970 reduced sulfur in Everglades dissolved organic matter controlled by
971 sulfate enrichment. *Environmental Science & Technology*, *51*(7), 3630–
972 3639. https://doi.org/10.1021/acs.est.6b04142
973 Poulin, B. A., Ryan, J. N., Tate, M. T., Krabbenhoft, D. P., Hines, M. E., Barkay,
974 T., Schaefer, J., & Aiken, G. R. (2019). Geochemical factors controlling
975 dissolved elemental mercury and methylmercury formation in Alaskan
976 wetlands of varying trophic status. *Environmental Science &*
977 *Technology*, *53*(11), 6203–6213.
978 https://doi.org/10.1021/acs.est.8b06041
979 Roth, S., Poulin, B. A., Baumann, Z., Liu, X., Zhang, L., Krabbenhoft, D. P.,
980 Hines, M. E., Schaefer, J. K., & Barkay, T. (2021). Nutrient inputs
981 stimulate mercury methylation by syntrophs in a subarctic peatland.
982 *Frontiers in Microbiology*, *12*.
983 https://doi.org/10.3389/fmicb.2021.741523
984 Schaefer, J. K., Kronberg, R., Björn, E., & Skyllberg, U. (2020). Anaerobic
985 guilds responsible for mercury methylation in boreal wetlands of varied

trophic status serving as either a methylmercury source or sink. *Environmental Microbiology*, *22*(9), 3685–3699. https://doi.org/10.1111/1462-2920.15134

Schaefer, J. K., & Morel, F. M. M. (2009). High methylation rates of mercury bound to cysteine by *Geobacter sulfurreducens*. *Nature Geoscience*, *2*(2), 123–126. https://doi.org/10.1038/ngeo412

Schaefer, J. K., Rocks, S. S., Zheng, W., Liang, L., Gu, B., & Morel, F. M. M. (2011). Active transport, substrate specificity, and methylation of Hg(II) in anaerobic bacteria. *Proceedings of the National Academy of Sciences*, *108*(21), 8714–8719. https://doi.org/10.1073/pnas.1105781108

Sieber, J. R., McInerney, M. J., & Gunsalus, R. P. (2012). Genomic insights into syntrophy: The paradigm for anaerobic metabolic cooperation. *Annual Review of Microbiology*, *66*(1), 429–452. https://doi.org/10.1146/annurev-micro-090110-102844

Smith, S. D., Bridou, R., Johs, A., Parks, J. M., Elias, D. A., Hurt, R. A., Brown, S. D., Podar, M., & Wall, J. D. (2015). Site-directed mutagenesis of *hgcA* and *hgcB* reveals amino acid residues important for mercury methylation. *Applied and Environmental Microbiology*, *81*(9), 3205–3217. https://doi.org/10.1128/AEM.00217-15

Sorek, R., Zhu, Y., Creevey, C. J., Francino, M. P., Bork, P., & Rubin, E. M. (2007). Genome-wide experimental determination of barriers to

horizontal gene transfer. *Science*, *318*(5855), 1449–1452. https://doi.org/10.1126/science.1147112

Stamatakis, A. (2014). RAxML version 8: A tool for phylogenetic analysis and post-analysis of large phylogenies. *Bioinformatics*, *30*(9), 1312–1313. https://doi.org/10.1093/bioinformatics/btu033

Tada, Y., Marumoto, K., & Takeuchi, A. (2020). Nitrospina-like bacteria are potential mercury methylators in the mesopelagic zone in the East China Sea. *Frontiers in Microbiology*, *11*, 1369. https://doi.org/10.3389/fmicb.2020.01369

Tate, M. T., DeWild, J. F., Ogorek, J. M., Janssen, S. E., Krabbenhoft, D. P., Poulin, B. A., Breitmeyer, S. E., Aiken, G. R., Orem, W. H., & Varonka, M. S. (2023). *Chemical characterization of water, sediments, and fish from Water Conservation Areas and Canals of the Florida Everglades (USA), 2012 to 2019* [U.S. Geological Survey data release]. https://doi.org/10.5066/P976EGIX

Tjerngren, I., Karlsson, T., Björn, E., & Skyllberg, U. (2012). Potential Hg methylation and MeHg demethylation rates related to the nutrient status of different boreal wetlands. *Biogeochemistry*, *108*(1–3), 335–350. https://doi.org/10.1007/s10533-011-9603-1

Vairavamurthy, A., & Mopper, K. (1987). Geochemical formation of organosulphur compounds (thiols) by addition of $H_2S$ to sedimentary organic matter. *Nature*, *329*(6140), 623–625. https://doi.org/10.1038/329623a0

Wiener, J. G., Krabbenhoft, D. P., Heinz, G. H., & Scheuhammer, A. M. (2003). Chapter 16: Ecotoxicology of Mercury. In D. J. Hoffman, B. A. Rattner, G. A. Burton, & J. Cairns (Eds.), *Handbook of Ecotoxicology* (2nd ed., pp. 407–461). CRC Press.

Yu, R.-Q., Reinfelder, J. R., Hines, M. E., & Barkay, T. (2018). Syntrophic pathways for microbial mercury methylation. *The ISME Journal*, *12*(7), 1826–1835. https://doi.org/10.1038/s41396-018-0106-0

Zhang, J., Wang, F., House, J. D., & Page, B. (2004). Thiols in wetland interstitial waters and their role in mercury and methylmercury speciation. *Limnology and Oceanography*, *49*(6), 2276–2286. https://doi.org/10.4319/lo.2004.49.6.2276

Zhang, T., Kim, B., Levard, C., Reinsch, B. C., Lowry, G. V., Deshusses, M. A., & Hsu-Kim, H. (2012). Methylation of mercury by bacteria exposed to dissolved, nanoparticulate, and microparticulate mercuric sulfides. *Environmental Science & Technology*, *46*(13), 6950–6958. https://doi.org/10.1021/es203181m

Zhou, Z., Tran, P. Q., Breister, A. M., Liu, Y., Kieft, K., Cowley, E. S., Karaoz, U., & Anantharaman, K. (2022). METABOLIC: High-throughput profiling of microbial genomes for functional traits, metabolism, biogeochemistry, and community-scale functional networks. *Microbiome*, *10*, 33. https://doi.org/10.1186/s40168-021-01213-8